

## The Scattering of $\pi^+$ -Mesons on Hydrogen. I. Angular Distributions at Energies of 176, 200, 240, 270 and 307 MEV.

A. I. MUKHIN, E. B. OZEROV AND B. PONTECORVO  
*Institute of Nuclear Problems, Academy of Sciences, USSR*

(Submitted to JETP editor June 7, 1956)

J. Exptl. Theoret. Phys. (U.S.S.R.) 31, 371-385 (1956)

The angular distribution of  $\pi^+$ -mesons with energies of 176, 200, 240, 270 and 307 mev scattered from liquid hydrogen has been studied with the help of scintillation counters. The total interaction cross section of  $\pi^+$ -mesons and hydrogen has also been measured by the method of attenuation of the beam. At all energies, except 307 mev, the data can be well described by a function of the form  $d\sigma/d\Omega = a + b \cos \theta + c \cos^2 \theta$ .

### INTRODUCTION

At this time there are comparatively little accurate data on the angular distribution of  $\pi^+$ -mesons elastically scattered from hydrogen. Most of the published results pertain to energies less than 200 mev.<sup>1-5</sup> This situation can be explained by the difficulty involved in obtaining sufficiently intense and monoenergetic beams of positive  $\pi$ -mesons of high energy from circular accelerators. The measurement carried out to an energy of 400 mev with a diffusion chamber<sup>6</sup> is of little accuracy because of the small number of observed interactions. The scattering of 310 mev  $\pi^+$ -mesons from hydrogen has been studied recently by Grigor'ev and Mitin<sup>7</sup> with photographic plates.

The possibility of obtaining intense beams of positive  $\pi$ -mesons of high energy at the Institute for Nuclear Problems of the Academy of Sciences of the USSR appeared only after the extraction from the synchrocyclotron chamber of a beam of protons with

an energy of approximately 660 mev and a density  $\sim 10^9 / \text{cm}^2 / \text{sec}$ .<sup>8</sup>

In the present communication the results of work<sup>9</sup> on the study of the scattering of  $\pi^+$ -mesons from hydrogen at meson energies of 176, 200, 240, 270 and 307 mev are presented in detail. The measurements were made with the help of scintillation counters.

### BEAMS OF $\pi^+$ -MESONS

Beams of  $\pi^+$ -mesons were obtained by the bombardment of a polyethylene target with a proton beam extracted from the synchrocyclotron. Mesons, formed in the reaction  $p + p \rightarrow \pi^+ + d$  at an angle of  $9^\circ$  with the incident proton beam, were magnetically deflected to an angle of  $20^\circ$  and, passing through an iron collimator four meters thick with an internal diameter of 5 cm, struck the detecting equipment placed behind the principal shielding wall of the synchrocyclotron (Fig. 1).

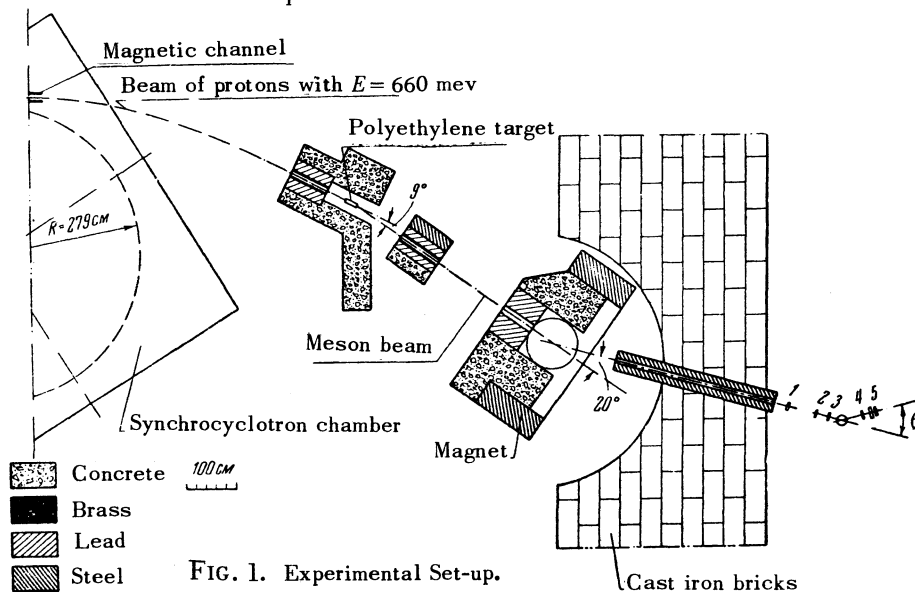


FIG. 1. Experimental Set-up.

For each desired meson energy, determined by the magnitude of the magnetic field of the deflecting magnet, the thickness of the polyethylene target was experimentally chosen in such a way as to obtain the maximum meson flux. The optimal thicknesses of the polyethylene target for energies of 176, 200, 240, 270 and 307 mev were, respectively, approximately 67, 53, 35, 19 and 4.6 gm/cm<sup>2</sup>. In these cases the obtained fluxes of mesons were approximately equal to 20, 40, 60, 60 and 40 cm<sup>-2</sup> sec<sup>-1</sup>.

It is interesting to note that despite the appreciable thicknesses of the targets used in these experiments there is a relatively narrow peak from the reaction  $p + p \rightarrow \pi^+ + d$  (Fig. 2) in the relation

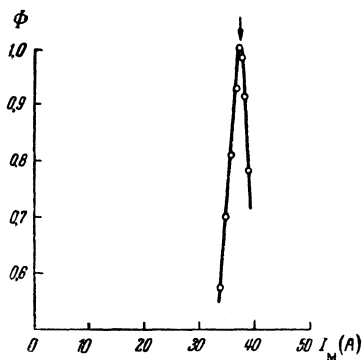


FIG. 2. Dependence of the intensity of the meson beam on the current in the deflecting magnet  $I_M$  for a polyethylene target thickness of 35 gm/cm<sup>2</sup>.  $E_\pi = 240$  mev.

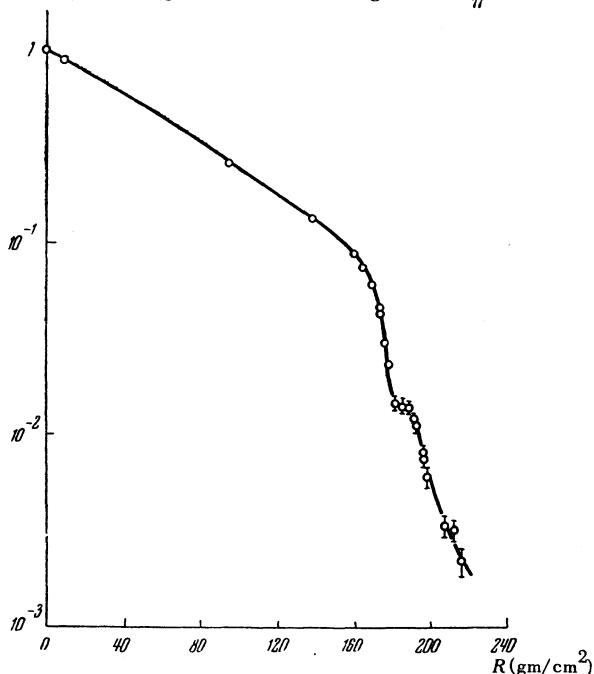


FIG. 3. Typical absorption curve ( $E_\pi = 307$  mev).

between the intensity of the meson beam,  $\Phi$ , and the current in the deflecting magnet,  $I_M$ . This

can be explained by the fact that mesons created in the forward part of the target and stopping in the target have approximately the same energy as mesons created by a slowed-down beam of protons in the "backward" part of the target, at their emergence from the target. The accurate determination of the energy in each case was carried out by measuring the range of mesons in copper. A typical absorption curve for 307 mev mesons is shown on Fig. 3. The range found from the curve was then corrected, as before,<sup>10</sup> for the calculated multiple Coulomb scattering of mesons in lead. For all energies this correction was approximately 2.5 % of the measured range and the energy essentially does not change due to the correction. To the "corrected" range was added 0.4 gm/cm<sup>2</sup> of copper, which is equivalent to the wall thickness of the photomultiplier container and the thickness of the plexiglass wall of the last scintillator. The final values of the energies, presented in Table 1, take into account the slowing down of mesons in the walls of the Dewar and in the hydrogen and correspond to the energy of the mesons in the center of the target. The uncertainty in the energy is due to the fundamental inaccuracy in the range determination, the initial inhomogeneity of the beam and also the inaccuracy in the calculation of the range-energy curve.

From the absorption curves and from known data on the nuclear interaction of  $\pi$ -mesons with copper, the admixture of  $\mu$ -mesons, which is also shown in Table 1, was determined.

## EXPERIMENTAL ARRANGEMENT

### A. ANGULAR DISTRIBUTION

The geometry of the experiment for the measurement of angular distributions is given in Fig. 4. In the experiments a Cerenkov counter, 1, was used as well as liquid scintillation counters 2 and 3, set in coincidence for the registration of the number of  $\pi^+$ -mesons hitting the hydrogen target (monitor). The Cerenkov detector was chosen in view of the fact that the meson beam contains an appreciable number of slow protons. The scattering of mesons from hydrogen was detected by liquid scintillation counters 4 and 5, set in coincidence with counters 1 and 3. The block diagram of the electronic equipment is shown on Fig. 5. The resolving time of the three-fold and four-fold coincidence schemes was equal to  $1.5 \times 10^{-8}$  sec. The stability of operation of the electronic equipment was systematically checked by the measurement of the ratio  $N_4 / N_3$ , the number of four-fold

TABLE I

Corrected range of $\pi^+$ -mesons in copper, in gm/cm <sup>2</sup>	Energy of the $\pi^+$ -mesons in the center of the hydrogenous scatterer, in mev	Uncertainty in the energy of the $\pi^+$ -mesons interacting with hydrogen, in mev	Percent admixture of $\mu^+$ -mesons
90.4	176	$\pm 4$	$4.7 \pm 1.5$
106.6	200	$\pm 5$	$4.0 \pm 1.0$
134.1	240	$\pm 6$	$3.7 \pm 1.0$
155.2	270	$\pm 6$	$3.4 \pm 1.0$
180.4	307	$\pm 6$	$2.6 \pm 1.0$

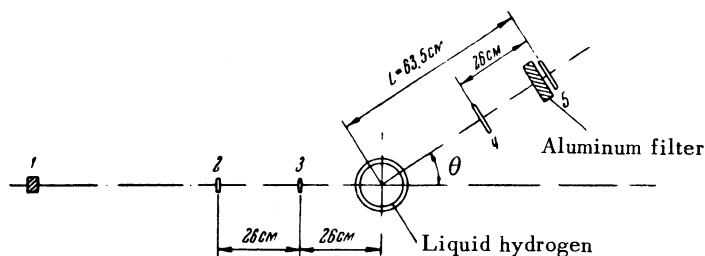


FIG. 4. Arrangement of the equipment used during the angular distribution measurements. 1—Cerenkov detector; 2,3,4,5—scintillation counters. For  $\theta = 20^\circ$ ,  $L = 73.5$  cm.

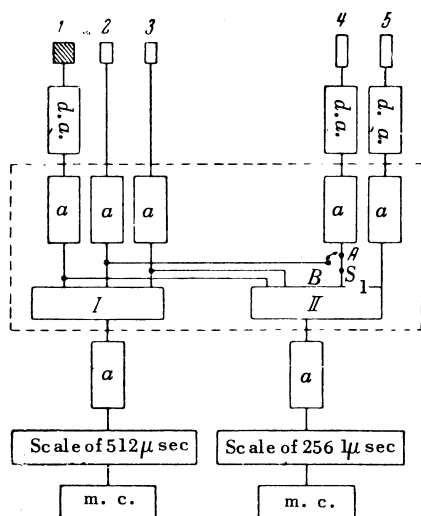


FIG. 5. Block diagram of the electronic equipment.  $S_1$  = switch. Differential cross sections were measured with the switch at point A (four-fold coincidences 1,3,4,5); total cross sections with the switch at point B (four-fold coincidences 1,2,3,5). A—amplifier, d.a.—distributing amplifier; I—3-fold coincidence scheme  $\sim 1.5 \times 10^{-8}$  sec; II—4-fold coincidence scheme  $\sim 1.5 \times 10^{-8}$  sec; 1—Cerenkov counter; 2,3,4,5—scintillation counters; m.c.—mechanical counter.

coincidences (1,3,4,5) and the number of three-fold coincidences (1,2,3) for which the counters 4 and 5 were set in one line with the counters 1,2 and 3.

Counter 1—the Cerenkov radiation detector—was built of plexiglass having dimensions of  $5 \times 5$  cm and a thickness of 3.6 cm and was connected by a plexiglass light pipe with a photomultiplier tube FEU-19. The scintillation counters 2 and 3 had dimensions  $5 \times 5 \times 0.6$  cm and consisted of a thin-walled plexiglass vessel filled with a solution of terphenyl in phenylcyclohexane. Counters 4 and 5 had a diameter and thickness of scintillating material (a solution of terphenyl in phenylcyclohexane) of 10 and 0.8 cm, respectively. The scintillators were connected by light pipes to photomultiplier tubes FEU-19.

A glass-walled Dewar with an internal diameter of about 14 cm and a wall thickness of  $1 \text{ gm/cm}^2$  was used for the hydrogen target. For a Dewar capacity of 3 liters and an average evaporation of the hydrogen of about  $0.25 \text{ l/hr}$ , uninterrupted work was assured for a period of 8 hours. During the experiments, the Dewar was pumped out for background determinations (without hydrogen).

It was assumed in determining the amount of hydrogen that the density of liquid hydrogen was  $0.0708 \text{ gm/cm}^3$ . Taking into account the fact that

the evaporation speed of the hydrogen was relatively small, the influence of bubbles on the density was neglected. The average amount of hydrogen in the path of the meson beam determined under the assumptions mentioned above was  $0.984 \text{ gm/cm}^2$  with an uncertainty of about 1%. In order not to register charged particles from stars formed in the walls of the Dewar or recoil protons from  $(\pi^+, p)$  scattering, an aluminum filter was placed between scintillators 4 and 5.

The angular distributions were obtained from the ratio  $N_4 / N_3$  after calculation of the detection efficiency of mesons under various angles and a number of other corrections which will be discussed in the next section.

### B. TOTAL CROSS SECTION

The total interaction cross section of  $\pi^+$ -mesons with hydrogen was measured by the absorption of the beam of mesons passing through the hydrogen scatterer in the geometry shown in Fig. 6.

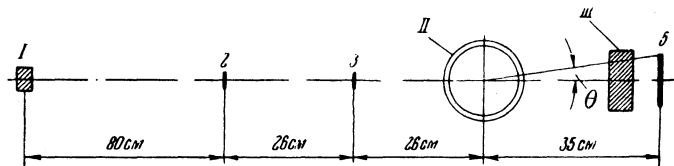


FIG. 6. Set-up of the equipment during the total cross section measurements. I—Cerenkov detector; 2,3,5—Scintillation counters; II—Dewar with liquid hydrogen, III— $\text{CH}_2$  filter (5 cm thick).

The differential cross section for the elastic scattering of  $\pi^+$ -mesons on hydrogen in the laboratory system was determined from the formula

$$\left(\frac{d\sigma}{d\Omega}\right)_{\text{lab}} = \left(\frac{N_4}{KN_3}\right) \left(\frac{1}{N_H \epsilon \Omega}\right),$$

where  $N_4$  is the number of registered four-fold coincidences of  $\pi^+$ -mesons scattered from hydrogen at a given angle  $\theta$ ;  $N_3$  is the number of three-fold coincidences;  $K$  is a factor characteristic of the beam;  $N_H$  is the number of hydrogen atoms per  $\text{cm}^2$ ;  $\epsilon$  is the detection efficiency for mesons at angle  $\theta$ ;  $\Omega$  is the effective solid angle. A discussion is presented below of experiments carried out to find the parameters entering in the formula shown above. The numerical values of the parameters will be shown in tables in which are presented the results of the measurements.

As in previous work on the determination of total cross sections, the distance between the center of the hydrogen scatterer and the last scintillator was equal to 35 cm, which corresponds to an average detection angle for the last detector of about  $8^\circ$ .

The beam of mesons falling on the hydrogen target was defined by the system of three counters 1, 2 and 3 set in coincidence. Having passed through the scatterer the beam was registered through a four-fold coincidence (1, 2, 3, 5). The block diagram of the electronic equipment for these experiments is also shown in Fig. 5.

The scintillators 2 and 3 used in these experiments had a diameter of 3 cm and a thickness of 0.4 cm and consisted of a thin-walled plexiglass container filled with a solution of terphenyl in phenylcyclohexane. The scintillator 5 had a diameter of 10 cm as before. The same hydrogen target was used as in the measurements of the angular distributions.

### THE METHOD OF THE MEASUREMENT OF ANGULAR DISTRIBUTIONS

#### A. DETERMINATION OF THE FLUX OF $\pi^+$ -MESONS

Because of the fact that in the scattering experiments a "thick" hydrogen target was used, it was necessary to take into account the absorption of the mesons not only in scintillator 3 and in the front walls of the Dewar but also in the hydrogen scatterer itself. In the determination of the number of mesons hitting the hydrogen target, counting errors in the counting scheme were taken into account; these occurred for relatively high intensities used in meson flux experiments, particularly for energies of 240 and 270 mev. Finally, it was necessary to consider the admixture in the beam of  $\mu$ -mesons which do not participate in nuclear interaction with hydrogen.

Taking into account the facts enumerated above, the average number of  $\pi^+$ -mesons,  $N_\pi = KN_3$ , which could participate in the scattering were determined in the following way:

$$N_{\pi} = KN_3 = N_3 \gamma \alpha_{\pi} \{1 - \frac{1}{2} \exp[-\sigma_t N_H] - \beta\}.$$

Here  $\eta$  is a coefficient which takes into account errors in counting during the registration of the number of three-fold coincidences;  $\alpha_{\pi}$  is the fraction of  $\pi$ -mesons in the beam;  $\sigma_t$  is the total interaction cross section of  $\pi^+$ -mesons with hydrogen;  $\beta$  is the fraction of the beam absorbed in scintillator 3 and in the front walls of the Dewar.

#### B. DETECTION EFFICIENCY OF THE MESONS

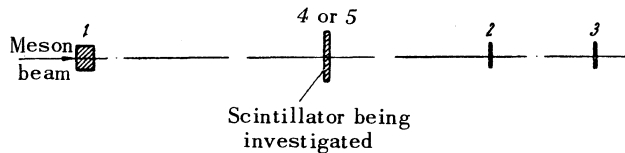


FIG. 7. Set-up of the experiment to determine the probability of the detection of mesons in scintillators 4 and 5.

It is found that the probability of detecting mesons in scintillators 4 and 5  $\epsilon_4 = N_4(1,2,3,4)/N_3(1,2,3)$  and  $\epsilon_5 = N_4(1,2,3,5)/N_3(1,2,3)$  were equal to unity with an accuracy of better than one percent.

The plateau of the system of the four counters 1,3,4 and 5 set up in a straight beam had a slope of the order of 1% per 200-300 volts.

To measure the absorption of scattered mesons in "equivalent filters" consisting of scintillator 4 and aluminum filters, counters 1,2,3 and 5 were

placed in a single line. The attenuation of meson beams in these equivalent filters was determined for a number of energies, using a variation of the electronic scheme (see Fig. 5) intended for the measurement of total cross sections. The geometry of the experiment is shown in Fig. 8. In these experiments the energy of the meson beam was set by the magnitude of the current in the deflecting magnet. The control measurement carried out by measuring the range in copper showed that the divergence between the energy values determined in both ways was less than  $\pm 2$  mev.

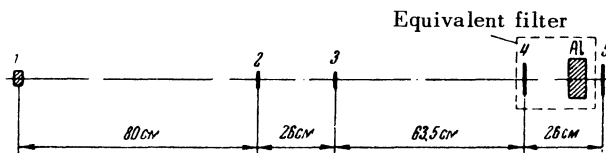


FIG. 8. Arrangement by which the attenuation of the meson beam in the filter was measured.

From the combined results, the measurements of

$$\epsilon_{\Phi} = \frac{N_4(\text{with filter})}{N_4(\text{without filter})} \text{ as a function of energy,}$$

taken for various thicknesses of the aluminum filter, show that for energies near 200 mev,  $\epsilon_{\Phi}(E)$  has a minimum, which can be understood from the character of the energy dependence of the total interaction cross section of  $\pi$ -mesons with complex nuclei.<sup>12</sup>

From the curves characterizing the absorption of mesons as a function of energy for various thicknesses of aluminum filter (Fig. 9), the detection efficiency for scattered mesons of a given energy was directly found, since the probability of detecting mesons traversing scintillators 4 and 5 is equal to unity. As a small correction to the detection efficiency the absorption of scattered mesons in the walls of the hydrogen target was taken into account. In such a way the detection efficiency of scattered mesons was determined to be

$$\varepsilon = \varepsilon_{\Phi} (1 - \kappa),$$

where  $\kappa$  is the fraction of scattered mesons absorbed in the Dewar walls.

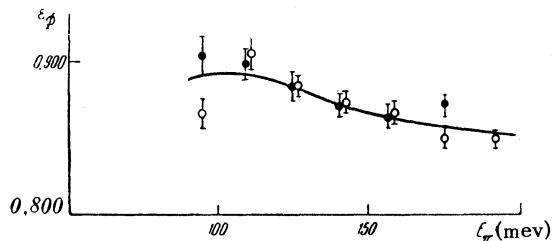


FIG. 9. Detection efficiency of mesons (for an aluminum filter thickness of 3 cm) as a function of energy.

### C. DETERMINATION OF THE EFFECTIVE SOLID ANGLE

The most substantial of the geometrical corrections depends on the fact that the dimensions of the scintillator 4 were less than the diameter of the hydrogen target. This leads to the fact that, depending on the angle, part of the hydrogen scatterer is in a half shadow with respect to the counter telescope 4-5; Fig. 10 shows the dependence on angle  $\theta$  of the ratio  $\Omega_{av} / \Omega_c$  where  $\Omega_c$  is the solid angle defined by scintillator 5 as seen from the center of the hydrogen target, and  $\Omega_{av}$  is the solid angle determined by the scintillation counter telescope 4-5, averaged with respect to the volume of the scatterer.

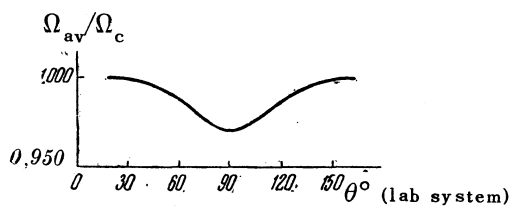


FIG. 10. Angular dependence of the quantity  $\Omega_{av} / \Omega_c$

In order to obtain the effective solid angle of detection of scattered mesons,  $\Omega$ , it is necessary to introduce a further correction to the quantity  $\Omega_{av}$ , taking into account the possibility of detecting scattered mesons in the light pipe of scintillation counter 5. The relatively large sensitivity of the plexiglass light pipe to high energy particles results

from Cerenkov radiation and from "feeble" scintillations in the plexiglass.

The increase of the average solid angle  $(\Omega - \Omega_{av}) \times \Omega_{av}$  was determined for mesons of known energy scattered through two angles. The relative dependence of the sensitivity of the light pipe on energy was determined in the direct meson beam for various values of the current in the deflecting magnet. This gave the possibility of obtaining the magnitude of the effective solid angle,  $\Omega$ , essential to the determination of the differential scattering cross section for mesons of various energies brought up in this work. The dependence of the increase of the average solid angle on the meson energy is shown in Fig. 11. In the determination of the effective solid angle a correction was also introduced due to the fact that the scintillation counter telescope has a finite angular resolution.

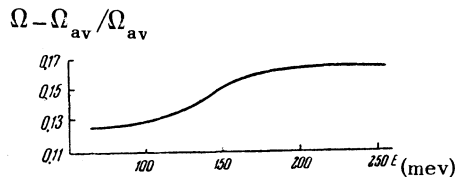


FIG. 11. Energy dependence of the quantity  $(\Omega - \Omega_{av}) / \Omega_{av}$ .

Processes of multiple nuclear scattering of mesons in hydrogen were not taken into account. Because of their small magnitude, corrections due to chance coincidence and  $\pi - \mu$  decay of scattered mesons were not taken into account.

### THE METHOD OF MEASUREMENT OF TOTAL CROSS SECTIONS

Total interaction cross sections of  $\pi^+$ -mesons with hydrogen, measured by the method of attenuation of the beam traversing the scatterer, were determined from the formula

$$\sigma_t(\pi^+, p) = \frac{1}{N_H} \ln \left\{ \frac{N_4^{(noH)} \eta^{(noH)} - N_4^{(0)} \eta^{(0)} \alpha_{\mu}}{N_4^{(H)} \eta^{(H)} - N_4^{(0)} \eta^{(0)} \alpha_{\mu}} \right\} + \int_0^{\theta_1} \left\{ \left( \frac{d\sigma_{\pi}}{d\Omega} \right)_{lab} + \left( \frac{d\sigma_p}{d\Omega} \right)_{lab} \right\} d\Omega.$$

The following terms are used here:  $N_4^{(0)}$ ,  $N_4^{(noH)}$  and  $N_4^{(H)}$  are respective to the number (having normalized to unity the reading of the monitor) of four-fold coincidence counts corresponding to the hydrogen free Dewar ( $N_4^{(0)}$ ), pumped out Dewar

( $N_4^{(\text{noH})}$ ) and Dewar filled with liquid hydrogen ( $N_4^{(\text{H})}$ );  $\eta^{(0)}$ ,  $\eta^{(\text{noH})}$  and  $\eta^{(\text{H})}$  are factors which take into account counting errors in the detecting apparatus,  $\alpha_\mu$  is the fraction of  $\mu$ -mesons in the beam;  $(d\sigma_\pi/d\Omega)_{\text{lab}}$  is the angular distribution of  $\pi$ -mesons in the laboratory system of coordinates;  $(d\sigma_\rho/d\Omega)_{\text{lab}}$  is the angular distribution of recoil protons in the laboratory system of coordinates;  $\theta_1 = 8^\circ$ .

Chance coincidences, determined in a separate experiment, were negligibly small (of the order of 0.1%) and were not taken into account.

## THE RESULTS OF THE MEASUREMENTS

### A. DIFFERENTIAL CROSS SECTIONS

The results of the measurements are presented in Tables 2–6. Besides the final values of the differential cross sections in the laboratory system  $(d\sigma/d\Omega)_{\text{lab}}$  and in the center-of-mass system  $(d\sigma/d\Omega)$ , previously determined numerical values of the parameters  $K$ ,  $\Omega$  and  $\epsilon$  are also given. One can obtain an idea of the magnitude of the background at various angles in the absence of hydrogen from the fourth column of Tables 2–6 where the ratio  $N_4(\text{Dewar})/N_4(\text{Dewar} + \text{H})$ , the number of four-fold coincidences normalized to unity on the monitor, is given. In the fifth column of these tables is shown the calculation  $[N_4(\text{Dewar} + \text{H}) - N_4(\text{Dewar})]$  of four-fold coincidences, dependent only upon hydrogen and normalized to  $10^6$  counts of the monitor, that is three-fold coincidences,  $N_3$ .

Errors in the final cross section results are standard deviations. They include errors in the determination of corrections and they have only a statistical nature in the final calculation.

In regard to other supplementary errors of unknown origin, it is seen that it is unlikely that they are of appreciable magnitude because of the closeness of the value of the total cross section  $\sigma_t(\pi^+, p)$ , determined independently by the attenuation of the meson beam, and the value of

$$\sigma_t = \int (d\sigma/d\Omega) d\Omega,$$

obtained by integrating the differential cross sections. However the presence of such errors indicate the magnitude of the deviation of the experimental points from the "best" curve computed by the method of least squares.

At first, after considering the obtained results, a very much simplified phase analysis was made in the belief that only  $S$ - and  $P$ -waves participate in the scattering, that is that the angular distributions have the form

$$d\sigma/d\Omega = a_0 + a_1 P_1(\cos \theta) + a_2 P_2(\cos \theta).$$

The corresponding coefficients for various energies, found by the method of least squares, are presented in Table 7. For ease in comparing the results of this work with results of measurements of angular distributions at other energies, usually shown in the form  $d\sigma/d\Omega = a + b \cos \theta + c \cos^2 \theta$ , the corresponding coefficients are given in Table 8.

In the last column of Table 7 the values of

$$M = \sum_i \left\{ \frac{f(\theta_i) - \sigma(\theta_i)}{\Delta\sigma(\theta_i)} \right\}^2,$$

are given where  $\sigma(\theta_i)$  are the measured differential cross sections at an angle  $\theta_i$  with an experimental error  $\Delta\sigma(\theta_i)$ ;  $f(\theta_i)$  is the value of the function  $a_0 + a_1 P_1(\cos \theta) + a_2 P_2(\cos \theta)$  at an angle  $\theta_i$  found by the method of least squares. In the next to the last column the expected value  $M'$  of this quantity is given; it is equal to the difference between the number of experimental points and the numbers of free parameters.<sup>13</sup> As can be seen from the Table, for energies of 176, 200 and 240 mev, the value of  $M$  is close to the expected value. For an energy of 307 mev,  $M$  appreciably exceeds  $M'$ . This is illustrated in Figs. 12–16 where, together with the experimental cross sections, distributions of the type

$$d\sigma/d\Omega = a_0 + a_1 P_1(\cos \theta) + a_2 P_2(\cos \theta)$$

are shown.

Hence, for a meson energy of 307 mev there is definite sense in approximating the experimental data with a function having a larger number of free parameters, that is, a function of the type

$$d\sigma/d\Omega = a_0 + a_1 P_1(\cos \theta) + a_2 P_2(\cos \theta) + a_3 P_3(\cos \theta) + a_4 P_4(\cos \theta).$$

This may mean that for energies of  $\sim 300$  mev meson-nucleon scattering processes are already difficult to describe by means of  $S$ - and  $P$ -waves alone. The importance of the  $D$ -wave contribution will be discussed later. Table 9 gives the angular distribution coefficients, found by the method of least

TABLE 2. Angular distribution of  $\pi^+$ -mesons scattered from hydrogen,  $E_\pi = 176 \pm 4$  mev.

Angle $\theta$ (lab system), in degrees	Distance from the center of the target to the last scintillator in cm	Thickness of the aluminum filter in cm	Approximate magnitude of the background $N_4$ (Dewar) $N_4$ (Dewar + H)	"Clean" effect from hydrogen (for 10 <sup>6</sup> counts of the monitor)	K, beam characteristic factor	$\Omega$ , effective solid angle in the lab system, in steradians	$\epsilon$ , detection efficiency of scattered mesons	$(d\sigma/d\Omega)_{lab}$ differential cross section in the lab system, in 10 <sup>-27</sup> cm <sup>2</sup> /sterad	Angle $\theta$ in the center-of-mass, in degrees	$d\sigma/d\Omega$ differential cross section in the center-of-mass system, in 10 <sup>-27</sup> cm <sup>2</sup> /sterad
30	63.5	3.8	0.4	308 ± 30	0.915	2.20 × 10 <sup>-2</sup>	0.835	31.1 ± 3.1	38.5	20.0 ± 2.0
45	63.5	3.0	0.2	221 ± 20	0.915	2.16 × 10 <sup>-2</sup>	0.858	22.1 ± 2.1	56.8	15.7 ± 1.5
60	63.5	3.0	0.14	129 ± 14	0.915	2.17 × 10 <sup>-2</sup>	0.867	12.7 ± 1.4	74.2	10.2 ± 1.1
75	63.5	3.0	-0.17	96 ± 11	0.915	2.13 × 10 <sup>-2</sup>	0.879	9.6 ± 1.1	90.4	8.8 ± 1.0
90	63.5	0.8	0.17	105 ± 13	0.915	2.10 × 10 <sup>-2</sup>	0.912	10.2 ± 1.3	105.6	10.8 ± 1.4
105	63.5	0.8	0.13	128 ± 14	0.915	2.10 × 10 <sup>-2</sup>	0.904	12.5 ± 1.4	119.5	15.3 ± 1.7
120	63.5	0.8	0.16	142 ± 15	0.915	2.11 × 10 <sup>-2</sup>	0.900	13.9 ± 1.5	132.9	19.3 ± 2.1
135	63.5	0.8	0.22	146 ± 15	0.915	2.13 × 10 <sup>-2</sup>	0.898	14.2 ± 1.5	145.3	21.8 ± 2.3
149	63.5	0.8	0.10	175 ± 16	0.915	2.15 × 10 <sup>-2</sup>	0.898	16.8 ± 1.5	157.2	27.9 ± 2.6

TABLE 3. Angular distribution of  $\pi^+$ -mesons scattered from hydrogen,  $E_\pi = 200 \pm 5$  mev.

Angle $\theta$ (lab system), in degrees	Distance from the center of the target to the last scintillator in cm	Thickness of the aluminum filter, in cm	Approximate magnitude of the background $N_4$ (Dewar) $N_4$ (Dewar + H)	"Clean" effect from hydrogen (for 10 <sup>6</sup> counts of the monitor)	K, beam characteristic factor	$\Omega$ , effective solid angle in the lab system, in steradians	$\epsilon$ , detection efficiency of scattered mesons	$(d\sigma/d\Omega)_{lab}$ differential cross section in the lab system, in 10 <sup>-27</sup> cm <sup>2</sup> /sterad	Angle $\theta$ in the center-of-mass, in degrees	$d\sigma/d\Omega$ differential cross section in the center-of-mass system, in 10 <sup>-27</sup> cm <sup>2</sup> /sterad
20	73.5	6.8	0.6	249 ± 21	0.930	1.68 × 10 <sup>-2</sup>	0.734	36.9 ± 3.2	26.3	22.1 ± 1.9
35	63.5	6.8	0.3	242 ± 16	0.931	2.23 × 10 <sup>-2</sup>	0.733	27.0 ± 1.9	45.3	17.5 ± 1.2
50	63.5	3.0	0.2	199 ± 12	0.960	2.22 × 10 <sup>-2</sup>	0.850	18.7 ± 1.2	63.5	13.6 ± 0.9
80	63.5	3.0	0.2	77.6 ± 6.4	0.949	2.18 × 10 <sup>-2</sup>	0.870	7.38 ± 0.75	96.5	7.13 ± 0.73
95	63.5	3.0	0.1	93 ± 11	0.930	2.13 × 10 <sup>-2</sup>	0.883	9.0 ± 1.1	111.2	10.2 ± 1.2
110	63.5	3.0	0.1	117.1 ± 8.3	0.964	2.14 × 10 <sup>-2</sup>	0.893	10.8 ± 0.8	125.8	14.1 ± 1.1
150	63.5	3.0	0.2	141 ± 10	0.940	2.18 × 10 <sup>-2</sup>	0.881	13.3 ± 1.0	157.4	22.8 ± 1.7



TABLE 4. Angular distribution of  $\pi^+$ -mesons scattered from hydrogen,  $E_\pi = 240 \pm 6$  mev.

Angle $\theta$ (lab system), in degrees	Distance from the center of the target to the last scintillator, in cm	Thickness of the aluminum filter, in cm	Approximate magnitude of the background ( $N_4$ (Dewar) / $N_4$ (Dewar + H))	"Clean" effect from hydrogen (for 106 counts of the monitor)	K, beam characteristic factor	$\Omega$ , effective solid angle in the lab system, in steradians	$\epsilon$ , detection efficiency of the scattered mesons	$(d\sigma/d\Omega)_{lab}$ , differential cross section in the lab system, in $10^{-27}$ cm <sup>2</sup> /sterad	Angle $\theta$ in the center-of-mass, in degrees	$d\sigma/d\Omega$ differential cross section in the center-of-mass system, in $10^{-27}$ cm <sup>2</sup> /sterad
20	73.5	9.0	0.6	267 ± 25	0.999	1.69 × 10 <sup>-2</sup>	0.704	38.4 ± 3.7	26.8	22.0 ± 2.1
35	73.5	6.8	0.2	166 ± 12	0.999	1.69 × 10 <sup>-2</sup>	0.749	24.6 ± 1.6	46.3	15.4 ± 1.0
35	63.5	6.8	0.3	174 ± 18	0.999	2.25 × 10 <sup>-2</sup>	0.823	13.3 ± 1.0	64.7	9.47 ± 0.68
50	63.5	3.0	0.3	155 ± 10	1.074	2.25 × 10 <sup>-2</sup>	0.862	5.00 ± 0.36	97.8	4.92 ± 0.35
80	63.5	3.0	0.3	59.7 ± 4.0	1.074	2.20 × 10 <sup>-2</sup>	0.865	5.10 ± 0.38	112.4	5.86 ± 0.44
95	63.5	3.0	0.2	60.4 ± 4.2	1.066	2.16 × 10 <sup>-2</sup>	0.877	5.10 ± 0.38	126.0	6.80 ± 0.51
110	63.5	3.0	0.3	97.5 ± 5.1	1.067	2.15 × 10 <sup>-2</sup>	0.900	8.12 ± 0.47	158.1	14.50 ± 0.84
150	63.5	3.0	0.2		1.038	2.19 × 10 <sup>-2</sup>				

TABLE 5. Angular distribution of  $\pi^+$ -mesons scattered from hydrogen,  $E_\pi = 270 \pm 6$  mev.

Angle $\theta$ (lab system), in degrees	Distance from the center of the target to the last scintillator, in cm	Thickness of the Aluminum filter, in cm	Approximate magnitude of the background ( $N_4$ (Dewar) / $N_4$ (Dewar + H))	"Clean" effect from hydrogen (for 106 counts of the monitor)	K, beam characteristic factor	$\Omega$ , effective solid angle in the lab system, in steradians	$\epsilon$ , detection efficiency of the scattered mesons	$(d\sigma/d\Omega)_{lab}$ , differential cross section in the lab system, in $10^{-27}$ cm <sup>2</sup> /sterad	Angle $\theta$ in the center-of-mass, in degrees	$d\sigma/d\Omega$ differential cross section in the center-of-mass system, in $10^{-27}$ cm <sup>2</sup> /sterad
20	73.5	9.8	0.6	210 ± 16	1.042	1.69 × 10 <sup>-2</sup>	0.689	29.4 ± 2.4	27.5	16.4 ± 1.3
50	63.5	3.8	0.3	104.6 ± 6.4	1.025	2.26 × 10 <sup>-2</sup>	0.827	9.24 ± 0.61	65.7	6.52 ± 0.43
80	63.5	3.0	0.4	29.3 ± 2.6	1.026	2.23 × 10 <sup>-2</sup>	0.848	2.57 ± 0.24	98.8	2.52 ± 0.23
95	63.5	3.0	0.4	21.9 ± 3.8	1.032	2.15 × 10 <sup>-2</sup>	0.859	1.94 ± 0.34	113.3	2.26 ± 0.40
110	63.5	3.0	0.3	37.1 ± 2.9	1.028	2.16 × 10 <sup>-2</sup>	0.871	3.25 ± 0.26	126.8	4.46 ± 0.36
149	63.5	3.0	0.4	45.2 ± 3.2	1.021	2.19 × 10 <sup>-2</sup>	0.880	3.90 ± 0.29	157.7	7.22 ± 0.54

TABLE 6. Angular distribution of  $\pi^+$  mesons scattered from hydrogen,  $E_\pi = 307 \pm 6$  mev.

Angle $\theta$ (lab system) in degrees	Distance from the center of the target to the last scin- tillator, in cm	Thickness of the aluminum filter, in cm	Approximate mag- nitude of the back- ground $N_4$ (Dewar) $N_4$ (Dewar + H)	"Clean" ef- fect from hydro- gen (for 106 counts of the monitor	K, beam charac- teristic factor	$\Omega$ , effective solid angle in the lab system, in steradians	$\epsilon$ , detection effi- ciency of the scattered mesons	$(d\sigma/d\Omega)_{lab}$ differential cross section in the lab system in $10^{-27}$ $cm^2/sterad$	Angle $\theta_{in}$ the center-of- mass, in degrees	$d\sigma/d\Omega$ differ- ential cross sec- tion in the center of mass system, in $10^{-27} cm^2/sterad$
20	73.5	14.0	0.6	186 $\pm$ 15	1.024	1.69 $\times$ 10 $^{-2}$	0.672	27.2 $\pm$ 2.3	27.9	14.5 $\pm$ 1.2
35	63.5	6.0	0.3	174 $\pm$ 17	0.984	2.25 $\times$ 10 $^{-2}$	0.804	16.6 $\pm$ 1.7	47.9	9.86 $\pm$ 0.99
50	63.5	5.0	0.3	96.1 $\pm$ 5.1	1.021	2.26 $\times$ 10 $^{-2}$	0.829	8.55 $\pm$ 0.48	67.1	5.91 $\pm$ 0.33
80	63.5	2.0	0.5	21.1 $\pm$ 2.2	1.021	2.25 $\times$ 10 $^{-2}$	0.908	1.72 $\pm$ 0.19	100.0	1.55 $\pm$ 0.17
95	63.5	3.0	0.4	22.8 $\pm$ 4.5	0.992	2.18 $\times$ 10 $^{-2}$	0.850	2.10 $\pm$ 0.44	114.5	2.49 $\pm$ 0.49
110	63.5	2.0	0.3	29.1 $\pm$ 2.6	1.021	2.19 $\times$ 10 $^{-2}$	0.906	2.44 $\pm$ 0.23	127.8	3.42 $\pm$ 0.32
130	63.5	3.0	0.3	26.0 $\pm$ 4.4	0.996	2.18 $\times$ 10 $^{-2}$	0.875	2.33 $\pm$ 0.40	144.0	3.92 $\pm$ 0.67
149	63.5	2.0	0.4	30.1 $\pm$ 3.2	1.020	2.19 $\times$ 10 $^{-2}$	0.915	2.50 $\pm$ 0.27	158.2	4.77 $\pm$ 0.52

TABLE 7. The scattering of  $\pi^+$  mesons from hydrogen. The coefficients of the angular distribution.

Energy of the mesons, in mev	$d\sigma/d\Omega = a_0 + a_1 P_1(\cos \theta) + a_2 P_2(\cos \theta)$			$\chi^{-2} d\sigma/d\Omega = A_0 + A_1 P_1(\cos \theta) + A_2 P_2(\cos \theta)$			Expected Value $M = n - m$	M
	$a_0$	$a_1$	$a_2$	$A_0$	$A_1$	$A_2$		
176 $\pm$ 4	15.86 $\pm$ 0.38	-0.84 $\pm$ 0.76	13.5 $\pm$ 1.1	1.926 $\pm$ 0.047	-0.102 $\pm$ 0.093	1.63 $\pm$ 0.13	6	1.7
200 $\pm$ 5	14.15 $\pm$ 0.29	1.04 $\pm$ 0.55	12.47 $\pm$ 0.82	1.996 $\pm$ 0.041	0.147 $\pm$ 0.078	1.76 $\pm$ 0.11	4	5.7
240 $\pm$ 6	10.12 $\pm$ 0.29	4.58 $\pm$ 0.57	9.95 $\pm$ 0.63	1.770 $\pm$ 0.050	0.80 $\pm$ 0.10	1.74 $\pm$ 0.11	4	4.4
270 $\pm$ 6	6.47 $\pm$ 0.25	4.73 $\pm$ 0.50	7.07 $\pm$ 0.50	1.300 $\pm$ 0.050	0.95 $\pm$ 0.10	1.42 $\pm$ 0.10	3	5.0
307 $\pm$ 6	5.45 $\pm$ 0.19	5.12 $\pm$ 0.38	6.18 $\pm$ 0.40	1.275 $\pm$ 0.045	1.199 $\pm$ 0.089	1.45 $\pm$ 0.09	5	11.3

TABLE 8. The scattering of  $\pi^+$ -mesons from hydrogen. The coefficients of the angular distribution.

Energy of the mesons, in meV	$d\sigma/d\Omega = a + b \cos \theta + c \cos^2 \theta$			$\lambda^{-2} d\sigma/d\Omega = A + B \cos \theta + C \cos^2 \theta$		
	a	b	c	A	B	C
	$10^{-27} \text{ cm}^2 / \text{sterad}^{-1}$					
176	$9.14 \pm 0.42$	$-0.84 \pm 0.76$	$20.2 \pm 1.6$	$1.11 \pm 0.05$	$-0.10 \pm 0.09$	$2.45 \pm 0.19$
200	$7.92 \pm 0.36$	$1.04 \pm 0.55$	$18.7 \pm 1.2$	$1.12 \pm 0.05$	$0.15 \pm 0.08$	$2.64 \pm 0.17$
240	$5.15 \pm 0.22$	$4.58 \pm 0.57$	$14.93 \pm 0.95$	$0.90 \pm 0.03$	$0.80 \pm 0.10$	$2.61 \pm 0.17$
270	$2.93 \pm 0.15$	$4.73 \pm 0.50$	$10.59 \pm 0.75$	$0.59 \pm 0.03$	$0.95 \pm 0.10$	$2.13 \pm 0.15$
307	$2.36 \pm 0.14$	$5.12 \pm 0.38$	$9.26 \pm 0.60$	$0.55 \pm 0.03$	$1.20 \pm 0.09$	$2.17 \pm 0.14$

TABLE 9. The scattering of  $\pi^+$ -mesons from hydrogen ( $E_\pi = 307 \text{ meV}$ ). The angular distribution coefficients.

$d\sigma/d\Omega = a_0 + a_1 P_1(\cos \theta) + a_2 P_2(\cos \theta) + a_3 P_3(\cos \theta) + a_4 P_4(\cos \theta)$				$\lambda^{-2} d\sigma/d\Omega = A_0 + A_1 P_1(\cos \theta) + A_2 P_2(\cos \theta) + A_3 P_3(\cos \theta) + A_4 P_4(\cos \theta)$				$M'$	$M$		
$a_0$	$a_1$	$a_2$	$a_3$	$a_4$	$A_0$	$A_1$	$A_2$			$A_3$	$A_4$
$10^{-27} \text{ cm}^2 / \text{sterad}^{-1}$											
$5.49 \pm 0.21$	$5.22 \pm 0.49$	$6.05 \pm 0.61$	$0.43 \pm 0.58$	$-1.34 \pm 0.52$	$1.285 \pm 0.049$	$1.22 \pm 0.11$	$1.42 \pm 0.14$	$0.10 \pm 0.14$	$-0.31 \pm 0.1$	3	1.4

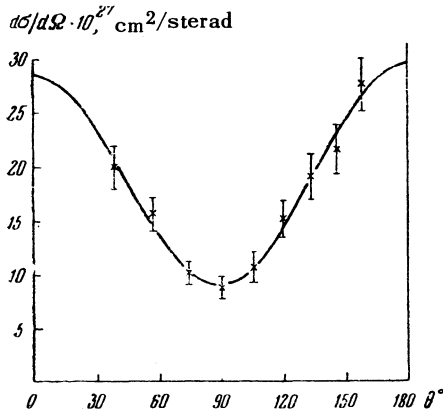


FIG. 12. Angular distribution of 176 mev  $\pi^+$ -mesons scattered from hydrogen. The full curve is for a distribution of the form  $d\sigma/d\Omega = [15.9 - 0.8 P_1(\cos \theta) + 13.5 P_2(\cos \theta)] \times 10^{-27} \text{ cm}^2/\text{sterad}$  with coefficients derived by the method of least squares.

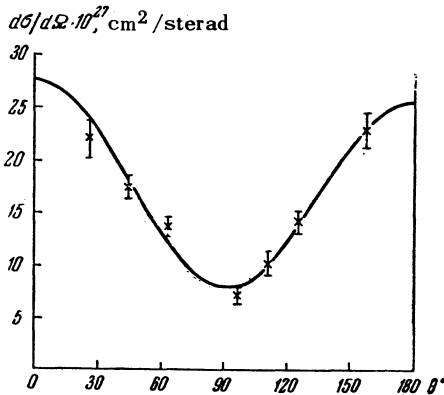


FIG. 13. Angular distributions of 200 mev  $\pi^+$ -mesons scattered from hydrogen. The full curve is for a distribution of the form  $d\sigma/d\Omega = [14.2 + 1.0 P_1(\cos \theta) + 12.5 P_2(\cos \theta)] \times 10^{-27} \text{ cm}^2/\text{sterad}$  with coefficients derived by the method of least squares.

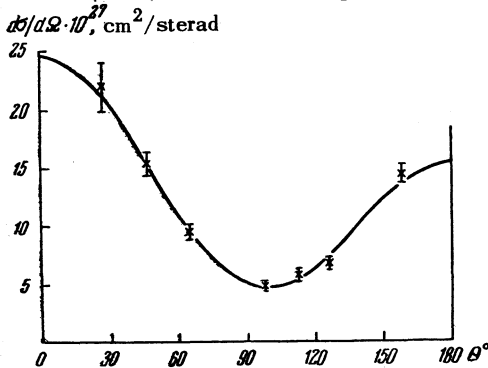


FIG. 14. Angular distribution of 240 mev  $\pi^+$ -mesons scattered from hydrogen. The full curve is for a distribution of the form  $d\sigma/d\Omega = [10.1 + 4.6 P_1(\cos \theta) + 9.9 P_2(\cos \theta)] \times 10^{-27} \text{ cm}^2/\text{sterad}$  with coefficients derived by the method of least squares.

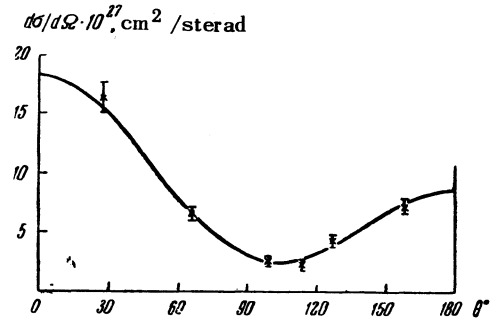


FIG. 15. Angular distribution of 270 mev  $\pi^+$ -mesons scattered from hydrogen. The full curve is for a distribution of the form  $d\sigma/d\Omega = [6.5 + 4.7 P_1(\cos \theta) + 7.1 P_2(\cos \theta)] \times 10^{-27} \text{ cm}^2/\text{sterad}$  with coefficients derived by the method of least squares.

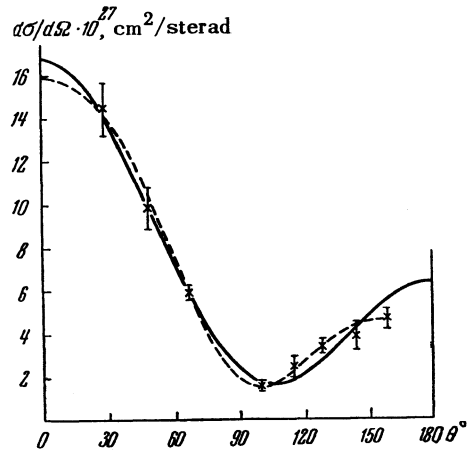


FIG. 16. Angular distribution of 307 mev  $\pi^+$ -mesons scattered from hydrogen. The full and the dashed curves correspond, respectively, to distributions of the form  $d\sigma/d\Omega = 5.5 + 5.1 P_1(\cos \theta) + 6.2 P_2(\cos \theta) \times 10^{-27} \text{ cm}^2/\text{sterad}$  and  $d\sigma/d\Omega = 5.5 + 5.2 P_1(\cos \theta) + 6.1 P_2(\cos \theta) + 0.4 P_3(\cos \theta) - 1.3 P_4(\cos \theta)$  with coefficients derived by the method of least squares.

squares, of the approximate function with five free parameters.

The dashed curve on Fig. 16 represents the distribution

$$d\sigma/d\Omega = [5.49 + 5.22P_1(\cos \theta) + 6.05P_2(\cos \theta) + 0.43P_3(\cos \theta) - 1.34P_4(\cos \theta)] \cdot 10^{-27} \text{ cm}^2/\text{sterad}.$$

#### B. TOTAL CROSS SECTIONS

The magnitudes of the total cross sections are given in Table 10. The errors shown are standard

TABLE 10. Total interaction cross section of  $\pi^+$ -mesons with hydrogen.

Meson energy, in mev	$\sigma_t(\pi^+, p)$ , $10^{-27} \text{ cm}^2$	$\int (d\sigma/d\Omega) d\Omega = 4\pi a_0$ , $10^{-27} \text{ cm}^2$	$\int (d\sigma/d\Omega) d\Omega = 4\pi a_0$ , $10^{-27} \text{ cm}^2$
$176 \pm 4$	$193 \pm 6^*$	$199.4 \pm 4.9$	$69.0 \pm 2.6$
$200 \pm 5$		$177.9 \pm 3.7$	
$240 \pm 6$	$125.6 \pm 2.5$	$127.2 \pm 3.6$	
$270 \pm 6$	$85.2 \pm 3.0$	$81.3 \pm 3.1$	
$307 \pm 6$	$65.7 \pm 2.2$	$68.5 \pm 2.4$	

\* Measurement made earlier at an energy of 174 mev (see Ref. 11).

deviations and include the uncertainty in the corrections, taking into account the finite solid angle subtended by the last counter, errors in counting in the registering equipment and the admixture of  $\mu$ -mesons. The contribution of the integral

$$\int_0^{\theta_1} \{ (d\sigma_\pi/d\Omega)_{\text{lab}} + (d\sigma_p/d\Omega)_{\text{lab}} \} d\Omega$$

to the total cross section constituted from  $4 \times 10^{-27}$  to  $6 \times 10^{-27} \text{ cm}^2$  with an uncertainty of the order of  $1 \times 10^{-27} \text{ cm}^2$  for all energies. The third and fourth column in the same table show the value of  $\int (d\sigma/d\Omega) d\Omega$  determined by the integration of the functions

$$a_0 + a_1 P_1(\cos \theta) + a_2 P_2(\cos \theta) \quad \text{and}$$

$$a'_0 + a'_1 P_1(\cos \theta) + a'_2 P_2(\cos \theta) + a'_3 P_3(\cos \theta) + a'_4 P_4(\cos \theta)$$

with coefficients which were given in Tables 8 and 9.

Together with the energy dependence of  $\sigma_t(\pi^+, p)$  found by the method of beam attenuation in this and in previous work,<sup>11</sup> Fig. 17 presents data found by integrating differential cross sections. As can be seen, the agreement of the magnitudes of the total cross sections appears good independently of the method used. There are some discrepancies only in the neighborhood of 200 mev. The comparison of these results with the data from other experiments<sup>14</sup> is carried out in the next paper which is devoted to discussion and interpretation of the results.<sup>15</sup>

The authors are pleased to thank B. S. Neganov who helped in obtaining the meson beam, and also V. V. Krotov for help with the work.

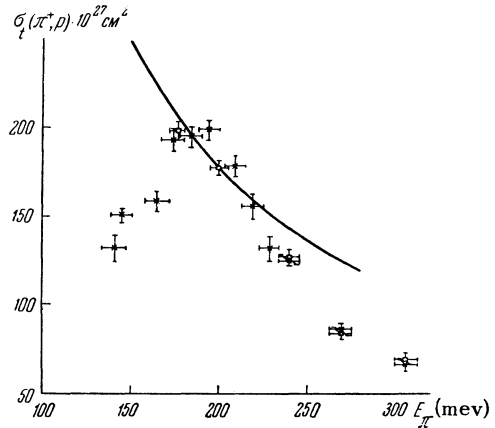


FIG. 17. Total interaction cross section of  $\pi^+$ -mesons with hydrogen from:  $x$ —the method of attenuation of the meson beam;  $\square$ —the integration of the angular distributions. The full curve shows the dependence of  $8\pi\lambda^2$  on energy.

<sup>1</sup>See, for instance, H. A. Bethe and F. de Hoffman, *Mesons and Fields* 2, 32 (1955).

<sup>2</sup>Ferretti, Manaresi, Puppi and Ranzi, *Nuovo Cimento* 1, 1238 (1955).

<sup>3</sup>J. Orear, *Phys. Rev.* 96, 1417 (1954).

<sup>4</sup>H. L. Anderson and M. Glicksman, *Phys. Rev.* 100, 268 (1955).

<sup>5</sup>Anderson, Davidson, Glicksman and Kruse, *Phys. Rev.* 100, 279 (1955).

<sup>6</sup>R. S. Margulies, *Bull. Amer. Phys. Soc.* 30, 28 (1955).

<sup>7</sup>E. L. Grigor'ev and N. A. Mitin, Report (Ochet) Institute for Nuclear Problems, Acad. of Sciences, USSR, 1955; paper at the International Conference on the Physics of High Energy Particles, May 14–22 (1956).

<sup>8</sup>Dmitrievskii, Danilov, Denisov, Zaplatin, Katyshev, Kropin and Chestnoi, paper at the International Conference on the Physics of High Energy Particles, May 14–22 (1956).

<sup>9</sup> Mukhin, Ozerov and Pontecorvo, Report (Otchet) Institute for Nuclear Problems, Acad. of Sciences, USSR, 1955; papers at the International Conference on the Physics of High Energy Particles, May 14–22 (1956).

<sup>10</sup> Ignatenko, Mukhin, Ozerov and Pontecorvo, Dokl. Akad. Nauk SSSR 103, 45 (1955).

<sup>11</sup> Ignatenko, Mukhin, Ozerov and Pontecorvo, J. Exptl. Theoret. Phys. (U.S.S.R.) 30, 7 (1956); Soviet Physics JETP 3, 10 (1956).

<sup>12</sup> Ignatenko, Mukhin, Ozerov and Pontecorvo, Dokl. Akad. Nauk USSR 103, 395 (1955).

<sup>13</sup> M. E. Rose, Phys. Rev. 91, 610 (1953).

<sup>14</sup> S. J. Lindenbaum and L. C. Yuan, Phys. Rev. 100, 306 (1955).

<sup>15</sup> A. I. Mukhin and B. Pontecorvo, J. Exptl. Theoret. Phys. (U.S.S.R.) 31, 550 (1956).

Translated by F. Ajzenberg—Selove  
78